Physica A 391 (2012) 819–827

Contents lists available at SciVerse ScienceDirect

Physica A

journal homepage: www.elsevier.com/locate/physa

The influence of connectivity on the firing rate in a neuronal network with electrical and chemical synapses

K.C. Iarosz [a], A.M. Batista [b], R.L. Viana [c,*], S.R. Lopes [c], I.L. Caldas [d], T.J.P. Penna [e]

[a] Pós-Graduação em Ciências, Universidade Estadual de Ponta Grossa, 84030-900, Ponta Grossa, Paraná, Brazil
[b] Departamento de Matemática e Estatística, Universidade Estadual de Ponta Grossa, 84030-900, Ponta Grossa, PR, Brazil
[c] Departamento de Física, Universidade Federal do Paraná, 81531-990, Curitiba, PR, Brazil
[d] Instituto de Física, Universidade de São Paulo, Caixa Postal 66316, 05315-970, São Paulo, SP, Brazil
[e] Universidade Federal Fluminense, Instituto de Ciências Exatas, INCT - Sistemas Complexos, Volta Redonda, RJ, Brazil

ARTICLE INFO

Article history:
Received 13 September 2011
Available online 22 September 2011

Keywords:
Neuronal networks
Chemical synapses
Electrical synapses
Cellular automata

ABSTRACT

We study the firing rate properties of a cellular automaton model for a neuronal network with chemical synapses. We propose a simple mechanism in which the nonlocal connections are included, through electrical and chemical synapses. In the latter case, we introduce a time delay which produces self-sustained activity. Nonlocal connections, or shortcuts, are randomly introduced according to a specified connection probability. There is a range of connection probabilities for which neuron firing occurs, as well as a critical probability for which the firing ceases in the absence of time delay. The critical probability for nonlocal shortcuts depends on the network size according to a power-law. We also compute the firing rate amplification factor by varying both the connection probability and the time delay for different network sizes.

1. Introduction

The human brain is a complex network that contains approximately 10^{11} neurons, each of them being connected with $\sim 10^4$ other neurons, on average. For example, one neuron in the vertebrate cortex may be connected to more than ten thousand post-synaptic neurons [1]. These properties make the brain a paradigmatic example of complex networks. Moreover, each neuron is a unit consisting of about a hundred specialized modules with different functions, each of them being a complex network itself, where each module receives excitatory inputs from a few thousands of other neurons [2].

In theoretical and computational studies where the Euclidean distance between neurons does not play a significant role, the corresponding networks may be treated from a graph–theoretical point of view [3]. However, if we regard the neurons as comprising a three-dimensional network (the brain, where they are connected by axons and dendrites), it is convenient to use a network embedded in an Euclidean space [4]. Due to this fact, it is often necessary to use models that exhibit spatiotemporal behavior.

Accordingly, neural network models are used to study biological neurons that are spatially distributed and are connected by both excitatory and inhibitory synaptic interactions, of both electrical and chemical nature [5]. For example, there are theoretical studies of the dynamics of networks with sparsely connected excitatory and inhibitory integrate-and-fire neurons [6]. It is possible to insert inhibitory connections in mathematical models through refractoriness or considering the dynamical units as being non-responsive during resting states until at least as many excitatory as inhibitory pulses are received [7].

* Corresponding author.
E-mail address: viana@fisica.ufpr.br (R.L. Viana).

0378-4371
doi:10.1016/j.physa.2011.09.014

The connection architecture of the mammalian nervous systems presents a large number of nonlocal shortcuts that connect spatially distant neurons, in such a way that the average distance between neurons is smaller than it would be in a network in which only nearest-neighbor interactions are considered. Moreover, we have also a high clustering, which characterizes this network as having the so-called *small-world* property [8,9]. Small-world networks have an average distance between sites comparable to the value it would take on a purely random network, while retaining an appreciable degree of clustering, as in regular networks [10]. Small-world networks have been considered as models of cortical networks following a number of neurophysiological evidences [11,12].

A realization of this concept was proposed by Watts and Strogatz, who introduced a small amount of randomness in an otherwise regular one-dimensional network with periodic boundary conditions [10]. This was done by re-wiring a small fraction of the local connections to new nodes randomly chosen along the network, so creating the shortcuts necessary to lessen the average distance between nodes. This procedure was proved to maintain a high amount of clustering, but it can also generate regions disconnected from the rest of the network, what would introduce divergent contributions to the average distance between nodes. It has been found that the small-world topology of the network connections may spontaneously induce periodic neural activity [13].

An alternative procedure was proposed by Newman and Watts [14], by the insertion of randomly chosen shortcuts in a regular network, instead of re-wiring local interactions into nonlocal ones. While the clustering properties of the Newman–Watts network are similar to the Watts–Strogatz ones, the above-mentioned problem of disconnectedness and infinite distances between nodes is circumvented. Since then, the Newman–Watts networks have been extensively used in a variety of theoretical and numerical studies on small-world networks [15].

The local dynamics of each network unit can be described by a variety of models, ranging from differential equations like the Hodgkin–Huxley [16] and Hindmarsh–Rose [17], to discrete-time maps [18–20]. In particular, two-dimensional maps with a few parameters are able to reproduce the essential dynamics presented in spiking neurons and other properties of excitable systems [20–23]. At the end of this spectrum we have cellular automata models for neural networks.

Cellular automata are simpler models than coupled map lattices and oscillator chains, since cellular automata are characterized by discrete space, time, and state variables [24]. The state variable of a cellular automaton takes on a set of discrete values at each spatial location and time instant. The state variables are updated simultaneously according to the values of the variables in their neighborhood, by using deterministic or stochastic rules. Cellular automata have been used to model a very wide variety of biological systems [25,26], such as the spread of epidemics [27], pattern formation and developmental biology [28], forest-fire models [29], neural dynamics [30,31], and cancerous growth [32]. In this work we choose to work with cellular automata due to their simplicity since we are to focus on small-world properties of the connection architecture rather in the local dynamics itself.

Under suitable conditions, the neurons in a cortical brain network fire collectively in a more or less synchronous way [33]. In complex networks characterized by small-world, scale-free or other architectures, it is important to determine under which conditions the neurons fire in a collective way. For example, since there are many randomly chosen shortcuts among neurons, one may wonder whether or not a given number of firing neurons are able to spread this effect along the network. We expect that the answer to this question relies on the statistical properties of the connection architecture. Moreover, since chemical synapses among neurons usually involve some threshold, there is an interplay between two effects: the connectivity of the network and the refractoriness characterizing the local dynamics of each neuron.

In this work we investigate a cellular automaton model for neuronal networks which include the small-world property in the connection architecture, by including randomly nonlocal connections according to a specified probability. The local dynamics in the cellular automaton consists of rules specifying how the state variables for each neuron are updated. We include the refractoriness property as the time delay that it takes for an individual neuron to be ready for firing again. These factors can be either antagonistic or cooperative due to the complex nature of the network, and our goal is to determine the dependence of the collective firing rate with both the connection and refractoriness properties.

The rest of this paper is organized as follows: in Section 2 we introduce the cellular automaton model for the individual neuron dynamics as well as the small-world model for the network architecture. Section 3 introduces the quantifiers we used to measure neuron activity and their significance. Section 4 shows the results that we obtained with respect to the dependence of the neuron activity with the time delay (refractoriness parameter). Section 5 considers the same kind of analysis, but with respect to the probability of nonlocal connections. The last section presents our Conclusions.

2. Neuronal network model

2.1. Local dynamics

The brain encodes, decodes and processes sensory and/or cognitive information through a neural code, which refers to the properties of a single sequence of action potentials (spike trains) or a spike train ensemble [34]. The basic mechanism of the neuron spiking is well known: a neuron cell in its resting state spikes only when suitably stimulated. After a spike, there is a refractory period during which further spikes cannot occur, until the cell returns to its resting state.

Hence a very simple description of the neuron activity assumes that it can be in two states: idle, when it is in a resting state, or spiking. Moreover, after it spikes, a neuron does not return immediately to the resting state due to the refractoriness period, which is taken to be the only parameter characterizing the local neuron dynamics.

Given these simplifying assumptions, we can use a cellular automaton to model the local neuron dynamics. Let $x_i(t)$, $i = 1, 2, \ldots, N$ be the state variable characterizing the ith neuron in a network at discrete time $t = 0, 1, 2, \ldots$. The state variable x_i is equal to zero if the neuron is in a resting (or idle) state, and different from zero if it spikes, assuming $\mu - 1$ different possible values $\{1, 2, \ldots, \mu - 1\}$, where μ is an integer. Only the state with $x_i = 1$ is considered as active, or firing, whereas the states with $2 \leq x_i \leq \mu$ are refractory, i.e. they cannot fire even if the external conditions are favorable for it.

Moreover, provided the neuron is in a resting state, it spikes as long as it receives a suitable external stimulus through its synapses, the effect of which will be modeled by the variable h_i. If $h_i = 0(1)$ the ith neuron does not receive (receives) any stimulus. After a neuron spikes, it takes a time delay $\tau - 2$ to exit its refractory period and return to the former resting state. A cellular automaton modeling these features is [25]

1. If $x_i(t) = 0$, then $x_i(t + 1) = h_i(t)$, where $h_i(t)$ can be equal to 0 or 1.
2. If $x_i(t) \neq 0$, then $x_i(t + 1) = [x_i(t) + 1],\ \mathrm{mod}\ \mu$, where $x_i(t) \in \{0, 1, \ldots, \mu - 1\}$ is the state of the ith cell at time t.

In other words, if there are stimuli ($h_i = 1$) when the cell is in its resting state ($x_i = 0$) then it spikes ($x_i = 1$), remaining insensitive during $\mu - 2$ further time steps.

The stimuli is represented by an external input signal $I_i(t)$ arriving on cell i at time t, which is modeled by a stochastic process of supra-threshold events of stereotyped unit amplitude [25]

$$I_i(t) = \sum_{\mu} \delta(t, t_{\mu}^{(i)}), \tag{1}$$

where $\delta(a, b)$ is the Kronecker delta and the time intervals $t_{\mu+1}^{(i)} - t_{\mu}^{(i)}$ are distributed exponentially according to a Poisson distribution with average (input rate) r.

An uncoupled cell presents $h_i(t) = \delta(I_i(t), 1)$, while a cellular automaton with N cells is governed by the equations

$$h_i(t) = 1 - [1 - \delta(I_i(t), 1)] \prod_{j=\pm 1} \left[1 - \delta(x_{i+j}(t), 1)\right]. \tag{2}$$

Summing up, the stimuli $h_i(t)$ will be nonzero whenever two of the following conditions as fulfilled: (i) one or more neighbors of the i-th cell are spiking; (ii) the external input on this neuron is nonzero. The cell responses vanish if the external inputs cease [31]. This representation is one variation of the mathematical model proposed by Greensberg and Hastings, that it was initially considered to analyze pattern formation in excitable media [35].

2.2. Connection architecture

We analyze a cellular automaton in that we insert shortcuts in an otherwise regular coupling so as to yield a small-world behavior, according to the Newman–Watts prescription, as commented in the Introduction. In our version of the Newman–Watts network, appropriate to discuss neuronal networks, the local connections represent the electrical (gap-junction) synapses and the shortcuts with time delay stand for the chemical synapses.

The model described by Eq. (2) and the corresponding updating rules does not consider nonlocal connections in its original form. Henceforth we will use (2) to model electrical (gap-junction) synapses, acting on the cells with random stimuli satisfying a stochastic process with Poisson distribution. However, for the chemical synapses the external inputs on the neurons (nonlocal connections) do not consider a random Poisson process, so that they are described by the following equation

$$h_i(t) = 1 - [1 - \delta(x_{i-1}(t), 1)]\,[1 - \delta(x_{i+1}(t), 1)] \prod_{j \in J} \left[1 - a_{ij}\delta(x_j(t - \tau), 1)\right], \tag{3}$$

where τ is the time delay and J is a set of nonlocal neighbors randomly chosen along the network according to a uniform probability distribution.

The last product in the Eq. (3) contains a non-symmetric connectivity matrix a_{ij}, whose entries are 0 and 1, randomly chosen according to a probability p (with uniform distribution). In Fig. 1 we represent such a network for only $N = 9$ neurons: the local connections among nearest-neighbors represent electrical (gap-junction) synapses, which are fast and bidirectional. The nonlocal connections, or shortcuts, stand for chemical synapses and are unidirectional. Hence the connectivity matrix representing chemical synapses is not symmetric.

For low values of the shortcut probability p the connectivity matrix is sparse. As an example, the nonlocal connectivity matrix related to the network depicted in Fig. 1 is

$$\begin{pmatrix} 0 & 0 & 0 & 0 & 0 & 0 & 0 & 0 & 0 \\ 0 & 0 & 0 & 0 & 0 & 0 & 0 & 0 & 0 \\ 0 & 0 & 0 & 0 & 0 & 0 & 0 & 1 & 0 \\ 0 & 1 & 0 & 0 & 0 & 0 & 0 & 0 & 0 \\ 0 & 0 & 0 & 0 & 0 & 0 & 0 & 0 & 0 \\ 0 & 1 & 0 & 0 & 0 & 0 & 0 & 0 & 0 \\ 0 & 0 & 0 & 0 & 0 & 0 & 0 & 0 & 0 \\ 0 & 0 & 0 & 0 & 0 & 0 & 0 & 0 & 0 \\ 0 & 0 & 0 & 0 & 0 & 0 & 0 & 0 & 0 \end{pmatrix}. \tag{4}$$

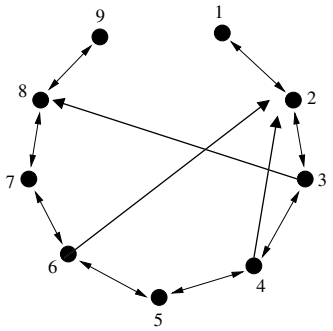

Fig. 1. Schematic representation of a small-world network of the Newman–Watts time with $N = 9$ nodes and free boundary conditions.

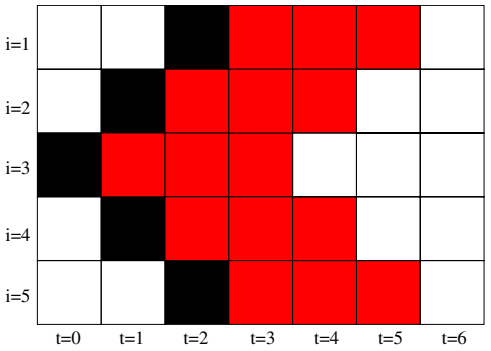

Fig. 2. (Color online) Time evolution of a a cellular automaton with $N = 5$ neurons with local connections only and $\mu = 5$ refractory states. Black squares represent $x_i = 1$, red squares $2 \leq x_i \leq 4$, and white squares $x_i = 0$.

We used free boundary conditions in numerical simulations: the end nodes x_1 and x_N have just one local link, and no nonlocal links at all (cf. Fig. 1), or $x_0(t) = x_{N+1}(t) = 0$ for all times. Starting from an initial condition $(x_i(0))$ the system evolves in time through a sequence of patterns, which may or may not settle down into a homogeneous absorbing state $x_1(t) = \cdots = x_N(t) = 0$ characterized by the absence of neuron firing.

A typical time evolution of the cellular automaton described here is (without nonlocal connections) depicted in Fig. 2 for a network with $N = 5$ neurons, $\mu = 5$ active (firing) states and free boundary conditions. Black squares are used to paint those cells for which $x_i = 1$, red is used for those which have $2 \leq x_i \leq 4$, and white squares stand for idle cells where $x_i = 0$. The red cells are in their refractory period, during which they cannot fire, even in presence of favorable conditions. At each step t the automaton rules are applied, such that for $t > 5$ there are no values with $x_i > 0$. The convergence to the absorbing state is typically very fast for such small cellular automata.

3. Neuron activity

Two mechanisms have been proposed to explain the measure of the stimulus intensities that can be coded by neuronal activity. The first one is adaptation, in that neurons control their range of operation according to the statistics of the environmental stimulus [36,37]. The second one is the intrinsic variation of firing thresholds among a population of sensory neurons, which would allow them to cover a wide range of stimuli [38].

Both mechanisms can mainly contribute to an enhancement of the dynamic range of a neuronal network. Neither adaptation nor threshold variation requires interactions among neurons to work, that is, the dynamical process does not depend on the activity of other sensory neurons. Thus, if the above-mentioned mechanism were the only ones responsible for an enhancement of sensitivity and dynamic range of neural networks, there should be no significant change in those properties if lateral connections among neurons were blocked [39].

Deans and coworkers obtained experimental data for the response function of retinal ganglion cells of mice with respect to the light intensity [40]. Retinal ganglion cells are neurons located near the inner surface of eye's retina which transmit visual information to several regions in the thalamus, hypothalamus, and mesencephalon, or midbrain [41]. There has been found a class of retinal ganglion cells that responded with large dynamic range. When the same experiment was repeated with cells without electrical synapses however, it has been found that both sensitivity and dynamic range were reduced. Hence the observed effects might be due to the electrical synapses.

These experimental results motivate the study of chemical synapses through nonlocal connections in neuronal networks. The influence of chemical synapses thus may be regarded as a third mechanism to explain changes in sensitivity and

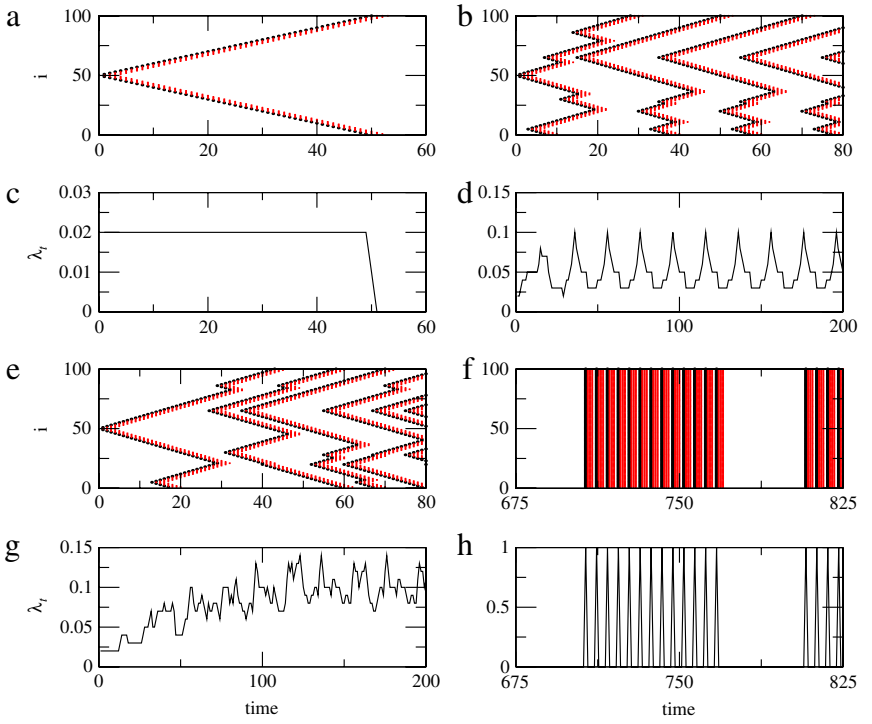

Fig. 3. (Color online) Spatiotemporal evolution of the neuron activity x_i for a cellular automaton model with (a) $p = 0$, $\tau = 0$ and (b) $p = 7 \times 10^{-4}$, $\tau = 0$. (c) and (d): density of excited neurons λ_t *vs.* time for (a) and (b), respectively. Spatiotemporal evolution of the neuron activity for (e) $p = 7 \times 10^{-4}$, $\tau = 10$ and (f) $p = 7 \times 10^{-4}$, $\tau = 100$. (g) and (h) density of excited neurons *vs.* time for (e) and (f), respectively. Black pixels correspond to $x_i = 1$ (firing state), red pixels to $2 \leq x_i \leq \mu - 1$ (refractory state), and white pixels to $x_i = 0$ (idle state). The remaining parameters are $N = 100$ and $\mu = 5$.

dynamical range due to neuronal activity. Recent work has indeed revealed that excitable neurons coupled via chemical or electrical synapses present enhanced sensitivity and dynamic range, as compared to those of isolated neurons [42–44].

Since the firing neurons, in our cellular automata model, are those cells with nonzero values of the state variable $x_i(t)$, it is useful to compute the density of excited neurons

$$\lambda_t \equiv \frac{1}{N} \sum_{i}^{N} \delta(x_i(t), 1), \tag{5}$$

in such a way that the neuron activity can be quantified by the firing rate, which is the time averaged density of firing neurons, or

$$F \equiv \frac{1}{T} \sum_{t}^{T} \lambda_t, \tag{6}$$

where T is a given time window for measurements.

4. Effect of the time delay

Initially we will discuss only locally coupled neurons without nonlocal connections. We plot in Fig. 3(a) the time evolution of the response (i.e., the state variable x) in a network with $N = 100$ cells, with the same palette used to represent the values of x as in Fig. 2. In this case there is no time delay $\tau = 0$ and we consider, as an initial condition, a spatial state in which $x_{50} = 1$, while all the other neurons are idle ($x_i = 0$, with $i \neq 50$). This corresponds to a single firing neuron located at the "midpoint" of the lattice.

From this initially active neuron there evolves an activity wave which dies off at the boundaries, due to the free boundary conditions we used, after which the network settles down in a homogeneous absorbing state of idle neurons. The corresponding density of excited neurons (Fig. 3(c)) is kept constant while this activity wave propagates through the network, and vanishes as we achieve this absorbing state.

Now let us consider the presence of nonlocal connections randomly chosen with a small probability $p = 7 \times 10^{-4}$ and a uniform distribution, but still without time delay, as before. The corresponding time evolution of the neuron activity is plotted in Fig. 3(b), for the same initial conditions as in the previous case. The activity wave generated by the firing neuron

no longer propagates for a long time along the network: it breaks down and suffers a series of interruptions before achieving the network boundaries, where it dies off.

On the other hand, new activity waves appear with a similar behavior, some of them with a short timespan. These patterns do not evolve to an absorbing state, as they did for purely local coupling. However, two activity waves can collide and cease locally neuron firing. Moreover, for some idle neurons there spontaneously appear a pair of activity waves. In fact, the corresponding density of excited neurons (Fig. 3(d)) presents a regular behavior exhibiting maxima and minima, as a result of these processes of creation and annihilation of activity waves.

Nonlocal connections (representing chemical synapses in the neuronal network model) are important to ensure that the network activity does not simply die out for long times. Furthermore the density of excited neurons in this case is periodic enough to allow for the coding of information. Such a self-sustained periodic behavior has been observed in small-world networks modeling the spread of infections [45,46]. Collective oscillations of this kind have been observed not only in small-world networks of excitable cellular automata, but also in random graphs that can be obtained through a network with small-world properties [47–49].

Now we consider the presence of time delay in the network with both local and nonlocal connections. In Fig. 3(e) we follow the time evolution of the neuron activity for a network with the same shortcut probability as in Fig. 3(b) and (d), but now with a time delay of $\tau = 20$. While the activity waves are still there, with no equilibrium absorbing state, the time evolution of the neuron activity seems to be less regular than in absence of time delay. This observation is confirmed by the time evolution of the corresponding density of excited neurons, which presents aperiodic behavior (Fig. 3(g)).

Time delay is an ingredient which often leads nonlinear systems to display complex dynamical behavior. In particular, the existence of negative feedback loops in physiological systems generates complex periodic and chaotic rhythms [50]. On increasing further the time delay the previously aperiodic neuron activity appears regular again but intermittent (Fig. 3(f)), a fact also apparent from the corresponding behavior for the density of excited neurons, which exhibits a bursting regime characterized by repeated firing (Fig. 3(h)).

This introduces two time scales in our system: a fast timescale characterized by the spiking, or firing activity itself; and a slow timescale related to the bursting. It is remarkable that this two-scale behavior, which is typically observed in differential equations and map-based neural models [51] can also be mimicked by simpler models, like cellular automata.

5. Effect of the shortcut probability

The neuron responses we describe by our model do not necessarily vanish if the external inputs cease, due to the fact that nonlocal couplings are capable to produce self-sustained activity. This result has been observed previously in a model developed by Copelli and coworkers [31]. In addition, such self-sustained activity was studied in great detail in a model of excitable integrate-and-fire neurons, both numerically and analytically [52,53].

When nearest-neighbor interactions are absent there is a minimum density of shortcuts such that persistent neuron activity is possible. The dynamics of cellular automata, like that considered here, is similar to that of integrate-and-fire neurons, provided these systems are coupled in a small-world network. We have observed a different behavior when the probability increases for high values of the delay, inasmuch as the average firing rate presents a constant value.

The dependence of the neuron activity in the cellular automaton model with the probability of nonlocal shortcuts can be quantified by using two measures: (i) the average firing rate *per* neuron $\langle F\rangle$ in the coupled system; and (ii) the average firing rate *per* neuron (denoted by $\langle f\rangle$) without the local coupling, i.e. considering *only* the nonlocal connections. The difference between $\langle F\rangle$ and $\langle f\rangle$, wherever it exists, is thus an evaluation of the effect of local connections on the neuron activity in the entire network. If $\langle f\rangle$ is greater (smaller) than $\langle F\rangle$, then the dominant influence on the firing rates is due to the nonlocal (local) connections.

The influence of the shortcut probability p on the average firing rates with and without nonlocal connections is analyzed in Fig. 4. In Fig. 4(a), obtained without time delay ($\tau = 0$), both average firing rates take on significant values only for a limited range of the nonlocal shortcut probability p. For small values of p the average firing rate $\langle F\rangle$ (black circles in Fig. 4) is higher than $\langle f\rangle$ (red squares in Fig. 4) since the dominant effect is from the local connections therein.

Higher values of p, on the other hand, stand for a stronger contribution of nonlocal shortcuts, and thus $\langle f\rangle$ is typically higher than $\langle F\rangle$ in such cases. Moreover, for large p there are global coupling effects that bring the system to an absorbing idle state and, accordingly, the firing rates there asymptote to zero. We thus define a critical probability p_c as the smaller value of shortcut probability such that the average firing rate is null, provided $\langle F\rangle$ decreases. An inspection of Fig. 4(a) shows that, in this case, $p_c \sim 0.1$, since before this value $\langle F\rangle$ is decreasing and, after this value $\langle F\rangle$ vanishes. For $p > p_c$ and $\tau = 0$, the average firing rate is null due to the onset of global behavior in the neuronal network.

When we consider a nonzero time delay (Fig. 4(b)) we observe that the network does not present a critical probability due to the self-sustained activity already mentioned in Fig. 3. Thus even large shortcut probabilities are not able to bring the network to an absorbing idle state, what is highly desirable from the neuroarchitectural point of view, since it represents a robust self-sustained firing behavior for a wide range of p-values. This observation is still valid when larger time delays are considered (Fig. 4(c)).

On the other hand, in this case the average firing rate of the local connections only ($\langle f\rangle$, represented by red circles) is nearly zero for all values of p, indicating that the larger time delay has brought the system to a state where the nonlocal shortcuts are relatively non-relevant, even though the corresponding probability p may be large. Furthermore, since the average firing

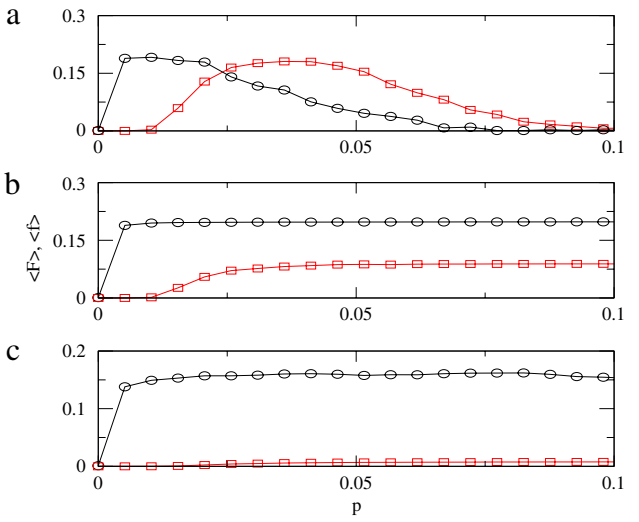

Fig. 4. (Color online) Average firing rate *per* neuron $\langle F \rangle$ (black circles) and average firing rate per neuron $\langle f \rangle$ for nonlocal connections only (red squares) as a function of the shortcut probability p, for 200 different realizations of the connectivity matrix and 1000 time instants. We considered a cellular automata with $N = 100$, $\mu = 5$, and: (a) $\tau = 0$, (b) $\tau = 10$ and (c) $\tau = 100$.

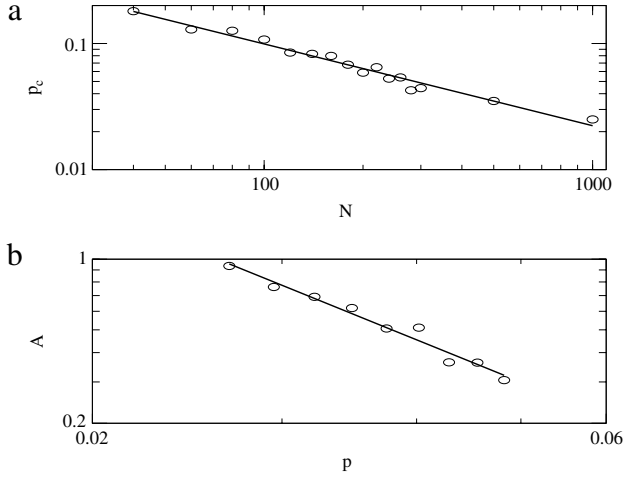

Fig. 5. (a) Critical probability of shortcuts as a function of network size; (b) amplification factor as a function of the shortcut probability. The full lines are least-squares fits. The time delay is zero and the remaining network parameters are the same as in the previous figures.

rate ($\langle F \rangle$) presents a constant value ($\sim$0.15) there is no dependence of the critical probability p_c on the shortcut density for high values of the time delay.

We found numerically that, for a network with both local and nonlocal connections and no time delay, the critical probability p_c decreases when the network size N increases (Fig. 5(a)), showing a power-law decrease $p_c \sim N^{\varpi}$, with $\varpi = -0.69 \pm 0.03$. This result is qualitatively similar to that observed in networks without nearest-neighbor interactions, for which the onset of neuron activity arises for $p \sim 1/N$, due to the reinjection of activity through shortcuts into previously active neurons [52].

We conclude that a network with both local and nonlocal connections presents smaller values for the critical shortcut probability than a network of the same size but with nonlocal connections only. Moreover, on considering both local and nonlocal connections, neuron firing occurs for a shorter range of the shortcut probability p as the network size increases.

The different responses of the receptor neurons associated with the local and nonlocal connections can be quantified by the so-called amplification factor $A \equiv \langle F \rangle / \langle f \rangle$ which quantifies the relative contribution of the nonlocal connections in terms of the average firing rates. If A is greater (smaller) than 1, the firing rates are dominated by the nonlocal (local) connections.

We obtained the amplification factor considering several values of the shortcut probability within a determined range for a network with local and nonlocal connections, and where the average firing rate does not vanish (Fig. 5(b)). For a fixed network size of $N = 100$ we observed that the amplification factor as a function of the probability obeys a power-law

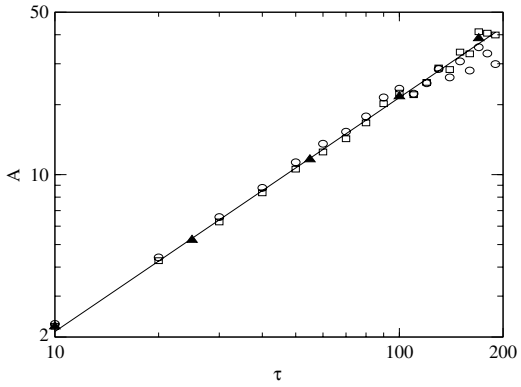

Fig. 6. Amplification factor as a function of the time delay for a network with shortcut probability $p = 0.1$ and different network sizes: $N = 100$ (circles), $N = 500$ (squares) and $N = 1000$ (triangles). The solid line is a least-squares fit.

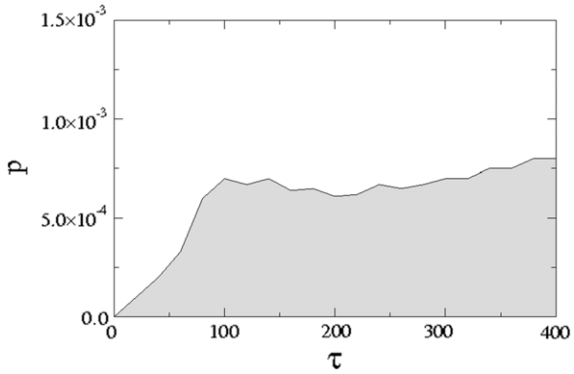

Fig. 7. Parameter plane (shortcut probability *vs.* time delay): the white region corresponds to self-sustained activity and the gray region to the vanishing of the firing rate (no activity).

$A \sim p^{\varsigma}$, where $\varsigma = -1.90 \pm 0.12$. This reflects the increasing importance (in terms of the firing rates) of nonlocal shortcuts as p increases, a result which is to be expected on general grounds.

The dependence of the amplification factor on the time delay is illustrated by Fig. 6 for three different values of the network size. The amplification factor increases with the time delay, the numerical results being fitted by a linear function ($A \sim \tau$), for network sizes ranging from $N = 10$ to 200. This means that the influence of the nonlocal shortcuts on the neuron firing is enhanced by the time delay, what explains why the red circles in Fig. 4(c) are more distant from the black circles in Fig. 4(b).

A further numerical experiment consists on investigating the ranges of the shortcut probability and time delays such that the network exhibits self-sustained firing activity (the opposite situation being the absorbing idle state in which the network does not exhibit activity at all). In order to investigate this dependence we considered, in Fig. 7, the parameter plane $p \times \tau$, in which the white region stands for self-sustained neuron activity, whereas the gray region represents the vanishing of the firing rate.

We drew in Fig. 7 a boundary line dividing such activity regions, using the following conditions: $\langle F \rangle > 0.9$ or $\langle F \rangle < 0.01$ for 10^4 time steps of the cellular automata. For small values of the shortcut probability ($p \lesssim 7 \times 10^{-4}$), self-sustained neuron activity ceases only if the time delay is large enough, up to $\tau \sim 100$. For larger shortcut probabilities, however, there seems not to exist a dependence between the probability to occur self-sustained neuron activity and the time delay, showing a kind of saturation effect: if the time delay is too large the system effectively loses memory of the previous behavior and the time delay effect turns not to be relevant.

6. Conclusions

In conclusion, we have presented a cellular automaton that models a neuronal network with both electrical and chemical synapses. The electrical (gap junction) synapses are modeled by local (nearest-neighbor) connections, whereas the chemical synapses are inserted in the model through shortcuts chosen in a probabilistic way so as to fulfill the properties of small-world networks: large clustering and small average distance between connected sites. The dynamics of a neuron is reduced to a description of its firing state, where we included a time delay which introduces a feedback mechanism. The latter is able to furnish a complex dynamical behavior for the model.

Accordingly, we observed that the connectivity properties of the network change the neuron firing rates, according to the probability of the nonlocal connections (shortcuts) that are probabilistically added to regular connections of the network. There is a range of values of the shortcut probability for which the firing rate does not vanish without a time delay. Increasing the shortcut probability leads to a critical value, after which neuron firing no longer occurs.

In addition, we showed that this critical probability depends on the network size. There is not a critical probability when the time delay is nonzero due to self-sustained activity displayed by the cellular automaton model. The network may present irregular or intermittent behavior for the density of excited neurons, depending on the coupling and dynamical properties.

An amplification factor was defined so as to measure the relative effect of the nonlocal connections on the network activity. This amplification factor was found to decrease when the shortcut probability increases. Moreover, we observed that the amplification factor increases with the time delay and that it does not depend on the network size, at least for the values used in our numerical simulations.

Acknowledgments

This work was made possible with the financial support of CNPq, CAPES, FAPESP, and Fundação Araucária.

References

[1] W. Gerstner, W.M. Kistler, Spiking Neuron Models, Cambridge University Press, Cambridge, 2002.
[2] M.F. Bear, B.W. Connors, M.A. Paradiso, Neuroscience: Exploring the Brain, second ed., Lippincott Williams & Wilkins, Philadelphia, 2002.
[3] P. Dayan, L.F. Abbott, Theoretical Neuroscience: Computational and Mathematical Modeling of Neural Systems, MIT Press, Cambridge, 2001.
[4] A.F. Rozenfeld, R. Cohen, D. Ben-Avraham, S. Havlin, Phys. Rev. Lett. 89 (2002) 218701.
[5] R.D. Traub, A. Bibbig, F.E.N. LeBeau, E.H. Buhl, M.A. Whittington, Ann. Rev. Neurosci. 27 (2004) 247.
[6] N. Brunel, J. Comput. Neurosci. 8 (2000) 183.
[7] R.D. Traub, R. Miles, R.K.S. Wong, Science 243 (1989) 1319.
[8] G. Zamora-López, C. Zhou, J. Kurths, Chaos 19 (2009) 015117.
[9] G. Zamora-López, C. Zhou, J. Kurths, Front. Neuroinform. 4 (2010) 1.
[10] D.J. Watts, S.H. Strogatz, Nature 393 (1998) 440.
[11] S. Achard, R. Salvador, B. Whitcher, J. Suckling, E. Bullmore, J. Neurosci. 26 (2006) 63.
[12] D.S. Basset, E. Bullmore, Neuroscientist 12 (2006) 512.
[13] D.R. Paula, A.D. Araújo, J.S. Andrade Jr., H.J. Herrmann, J.A.C. Gallas, Phys. Rev. E 74 (2006) 017102.
[14] M.E.J. Newman, D.J. Watts, Phys. Lett. A 263 (1999) 341.
[15] M.E.J. Newman, D.J. Watts, Phys. Rev. E 60 (1999) 7332.
[16] A. Hodgkin, A. Huxley, J. Physiology 117 (1952) 500.
[17] J.L. Hindmarsh, R.M. Rose, Proc. Royal Soc. London B 221 (1984) 87.
[18] N.F. Rulkov, Phys. Rev. Lett. 86 (2001) 183.
[19] N.F. Rulkov, Phys. Rev. E 65 (2002) 041922.
[20] B. Ibarz, J.M. Casado, M.A.F. Sanjuán, Phys. Rep. 501 (2011) 1.
[21] D.R. Chialvo, Chaos Solitons Fractals 5 (1995) 461.
[22] O. Kinouchi, M.H.R. Tragtenberg, Internat. J. Bifur. Chaos 6 (1996) 2343.
[23] S.M. Kuva, G.F. Lima, O. Kinouchi, M.H.R. Tragtenberg, A.C. Roque, Neurocomputing 38–40 (2001) 255.
[24] S. Wolfram, Rev. Modern Phys. 55 (1983) 3.
[25] M. Copelli, A.C. Roque, R.F. Oliveira, O. Kinouchi, Phys. Rev. E 65 (2002) 060901.
[26] Y.H. Zheng, Q.S. Lu, Physica A 387 (2008) 3719.
[27] G.Ch. Sirakoulis, I. Karafyllidis, A. Thanailakis, Ecol. Model. 133 (2000) 209.
[28] A. Deutsch, S. Dormann, Cellular Automaton Modeling of Biological Pattern Formation, Birkhäuser Verlag, Basel, 2004.
[29] P. Bak, K. Chen, C. Tang, Phys. Lett. A 147 (1990) 297.
[30] T. Takahashi, H. Oono, M.H.B. Radford, Physica A 387 (2008) 2066.
[31] M. Copelli, O. Kinouchi, Physica A 349 (2005) 431.
[32] A.-S. Qi, X. Zheng, C.-Y. Du, B.-S. An, J. Theoret. Biology 161 (1993) 1.
[33] P.J. Uhlhass, G. Pipa, B. Lima, L. Melloni, S. Neuenschwander, D. Nikolic, W. Singer, Front. Integrat. Neurosci. 3 (2009) 17.
[34] E.M. Izhikevich, Dynamical Systems in Neuroscience: The Geometry of Excitability and Bursting, The MIT Press, Boston, 2007.
[35] J.M. Greenberg, S.P. Hastings, SIAM J. Appl. Math. 34 (1978) 515.
[36] R.A. Normann, F.S. Werblin, J. Gen. Physiol. 63 (1974) 37.
[37] F.S. Werblin, J. Gen. Physiol. 63 (1974) 62.
[38] T.A. Cleland, C. Linster, Neural Comput. 11 (1999) 1673.
[39] T.L. Ribeiro, M. Copelli, Phys. Rev. E 77 (2008) 0519111.
[40] M.R. Deans, B. Volgyi, D.A. Goodenough, S.A. Boomfield, D.L. Paul, Neuron 36 (2002) 703.
[41] E. Kaplan, E. Bernadete, Progr. Brain Res. 134 (2001) 17.
[42] M. Copelli, P.R.A. Campos, Eur. Phys. J. B 56 (2007) 273.
[43] A.-C. Wu, X.-J. Xu, Y.-H. Wang, Phys. Rev. E 75 (2007) 032901.
[44] V.R.V. Assis, M. Copelli, Phys. Rev. E 77 (2008) 011923.
[45] M. Kuperman, G. Abramson, Phys. Rev. Lett. 86 (2001) 2909.
[46] P.M. Gade, S. Sinha, Phys. Rev. E 72 (2005) 052903.
[47] M. Girvan, D.S. Callaway, M.E.J. Newman, S.H. Strogatz, Phys. Rev. E 65 (2002) 031915.
[48] O. Kinouchi, M. Copelli, Nature Phys. 2 (2006) 348.
[49] F. Rozenblit, M. Copelli, J. Stat. Mech. 2011 (2011) P01012.
[50] L. Glass, A. Beuter, D. Larocque, Math. Biosci. 90 (1988) 111.
[51] C.A.S. Batista, S.R. Lopes, R.L. Viana, A.M. Batista, Neural Netw. 23 (2010) 114.
[52] A. Roxin, H. Riecke, S.A. Solla, Phys. Rev. Lett. 92 (2004) 198101.
[53] H. Riecke, A. Roxin, S. Madruga, S.A. Solla, Chaos 17 (2007) 026110.